EGYPTIAN DENTAL JOURNAL
www.eda-egypt.org
VOL. 69, 2643:2654, OCTOBER, 2023
PRINT ISSN 0070-9484 • ONLINE ISSN 2090-2360
ORAL SURGERY
Submit Date : 18-08-2023 • Accept Date : 27-08-2023 • Available online: 01-10-2023 • DOI : 10.21608/EDJ.2023.230060.2685

3D-PRINTED ZYGOMATIC SLIDING SURGICAL GUIDE: A NOVEL SURGICAL GUIDE, AN IN VITRO STUDY

Mohammed Hassan Al Kabany*

ABSTRACT

Objective: To assess the deviation of the fractured zygomatic bone involved in zygomaticomaxillary complex fractures after reduction using the proposed 3D-Printed Zygomatic Sliding Surgical Guide.

Material and methods: Twenty arbitrary zygomaticomaxillary complex fractures were virtually simulated on ten digital skulls. Individualized twenty 3D-Printed Zygomatic Sliding Surgical Guides and infraorbital and zygomaticofrontal plates were designed following the created fractures. The segmented skulls, zygomatic bones, surgical guides, and bone plates were 3D printed. The zygomatic bone was reduced into the planned position using the Zygomatic Sliding Surgical Guide. The reduced zygomatic bones were fixed at two points guided by the surgical guide using the 3D-printed bone plates. The reduced skull was scanned, and reduction was assessed at the four zygomatic bone tails.

Results: The zygomatic bones were reduced accurately into position with minimal mean deviations (0-0.6mm).

Conclusion: The proposed 3D-Printed Zygomatic Sliding Surgical Guide is valuable for reducing fractured zygomatic bones into virtually planned positions.

KEYWORDS: Zygomaticomaxillary complex fracture, surgical guide, reduction deviation, 3D printing.

INTRODUCTION

Zygomaticomaxillary complex (ZMC) is vital for facial skeleton function and appearance.[1] Following traumatic injuries, the nature of ZMC articulations results in complex fractures.[2] These fractures have several comorbidities[3] and substantial psychosocial effects[4]. Several factors are crucial for adequately managing ZMCFs. These factors are correct diagnosis, sufficient exposure, accurate anatomical reduction, adequate fixation, and follow-up.[5-7]

* Department of Oral and Maxillofacial Surgery, Faculty of Dentistry, Cairo University, Egypt.

Correct anatomical reduction of the ZMC is the keystone for functional and cosmetic restoration.[8-11] Traditionally, ZMCFs' reduction is based on the surgeon's mental simulation that varies according to experience and skills.[9,12-15] Which results in facial asymmetry requiring secondary intervention in 9% of all and 21% of comminuted ZMCFs.[16] Several methods were introduced to improve ZMCFs reduction. Including; virtual planning, surgical guides, intraoperative navigation, intraoperative imaging, and augmented reality.[17-20] 3D-printed surgical guides (3DP-SGs) were used in mandibular fractures, reconstruction, and orthognathic surgery.[19,21-23] However, few studies used 3DP-SGs to manage ZMCFs.[24,25] Moreover, the used surgical guides are conventional static (passive) stents.

The proposed 3D-printed Zygomatic Sliding Surgical Guide (3DP-ZSSG) was designed to actively reduce zygomatic bone in ZMCFs into virtually planned positions. It aids in manipulating the fractured zygoma and fixing the infraorbital plate in the intended location while stabilizing the bone in place. To the extent of the author's knowledge, 3DP-ZSSG is the first active surgical guide used in the management of maxillofacial fractures. The current study aimed to assess the degree of deviation of the fractured zygoma from the virtually planned position following reduction using the 3DP-ZSSG.

MATERIALS AND METHODS

An in-vitro study was done to assess the degree of reduction of zygomatic bone involved in ZMCFs utilizing the proposed 3DP-ZSSG. The study consisted of twenty 3DP-ZSSGs used to reduce twenty zygomatic bones of ten skulls.

Creation of 3D templates:

The 3D templates were designed in *SOLIDWORKS Professional* (2022, InspectionXpert Corporation, Germany) as follows. Infraorbital plate template (IO-PT): Six equally spaced circles (4.5mm diameter), each with an inner circle (1.8mm diameter), were created on a three-point arc and joint with connecting arcs. The skitch was extruded for 10mm. Zygomatico-frontal plate template (ZF-PT): ZF-PT was created as the IO-PT but with four cylinders. The infraorbital plate-track subtraction template (IO-PT-ST): The IO-PT sketch was offsite by 0.5mm and extruded for 10mm. (Fig1(a-f)) The threaded-column template (TCT): Thread cuts (metric die (M10X1.0), 1mm override pitch, 60° start angle, 2mm offset) were made on a cylinder (4mm base diameter, 20mm height). The nut: An inner cut thread (metric tap (M10X1.0), threads parameters as TCT) were made on a hexagon (across-sides width 6mm, 5mm height). The nut driver: a cylinder with an inner hexagon nut-hole (across-sides width 6.2mm, depth 15mm) was attached to a neck and a hexagon handle. (Fig2(a-g)) The designed models were exported as STL files.

Creation of skull and fractured zygoma:

A CT scan with an intact facial skeleton was uploaded to *Materialise Mimics Research software* (v21, Materialise NV Technologielaan, Belgium). Bone marrow spaces were filled, and the bone models were exported as an STL file and duplicated ten times; each was imported to a *Materialise 3-Matic Research* file (v13). Different arbitrary fracture lines segmented the zygomatic bone from the skull at the frontozygomatic tail (FZT) and zygomaticomaxillary (ZM) suture. (Fig3(a-d))

Bone plates adjustment:

The 3D templates were imported to the *3-Matic* file. The IO-PT and IO-PT-ST were oriented at the proposed site to bring their outer face parallel to and 4mm off the facial surface of the inferior orbital ridge (IOR). The IO-PT was subtracted from the skull duplicate into a 3mm thickness creating the infraorbital bone plate (IO-P). The same was done with the ZF-PT at the lateral orbital ridge crossing the fracture line creating the ZF bone plate (ZF-P) (Fig4a-d).

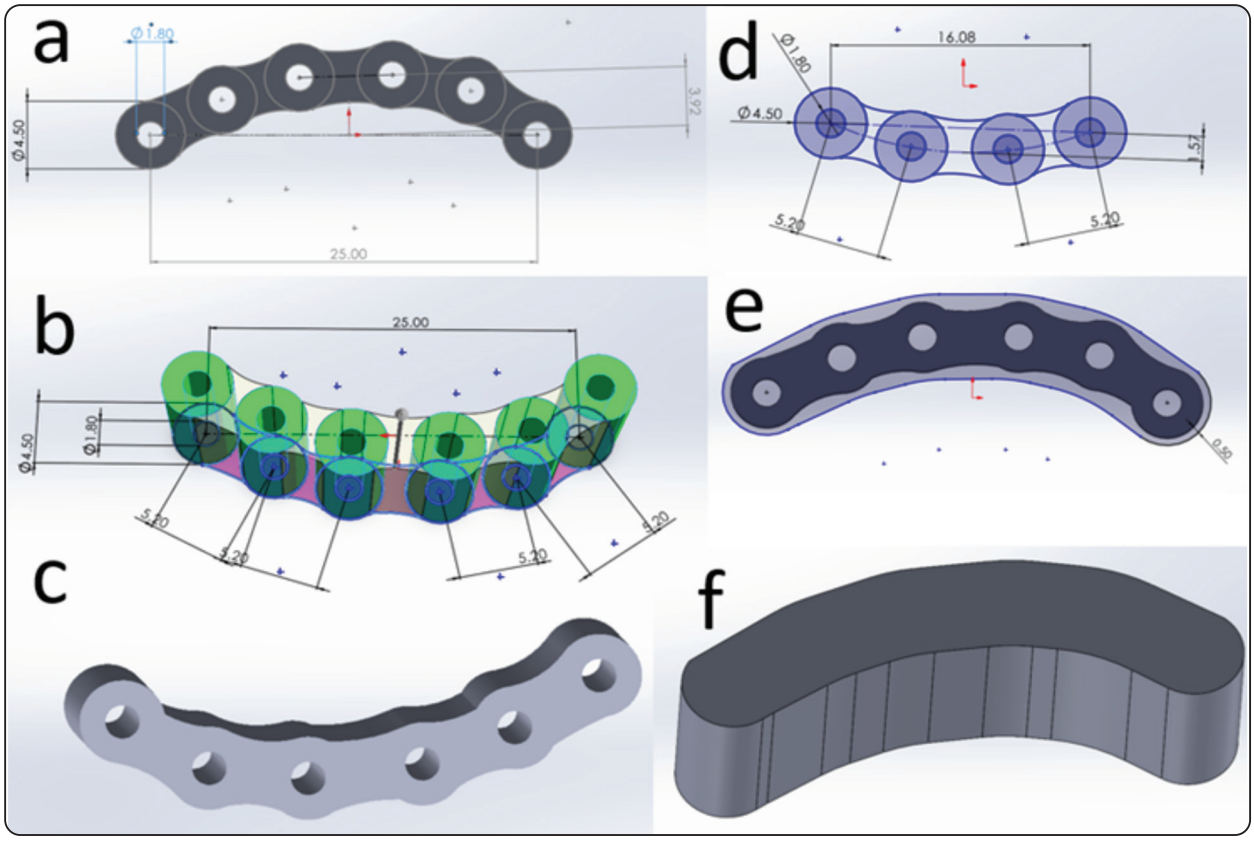

Fig. (1) a: IO-PT sketch; b: IO-PT sketch 10mm extrusion; c: IO-PT model; d: ZF-PT sketch; e: IO-PT-ST sketch; f: IO-PT-ST model.

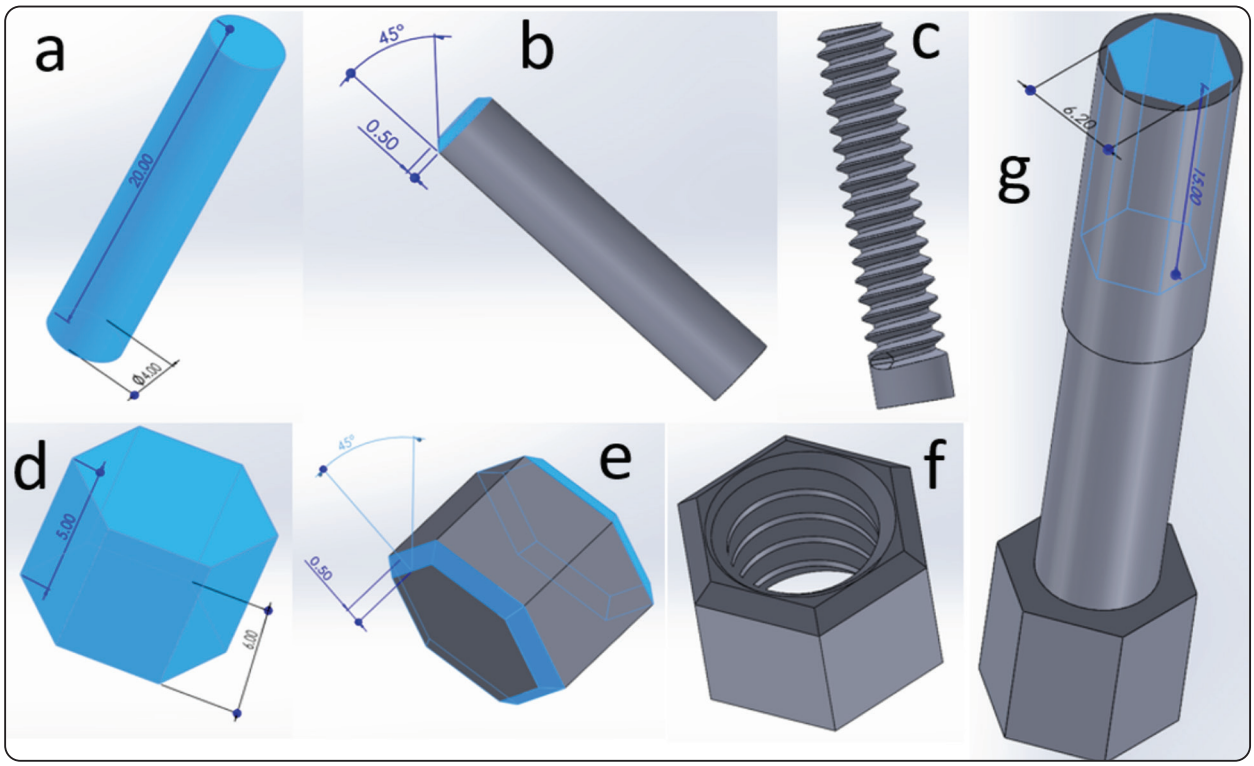

Fig. (2) a, b, & c: designing the TCT; d, e, & f: creating the nut; g: the nut driver.

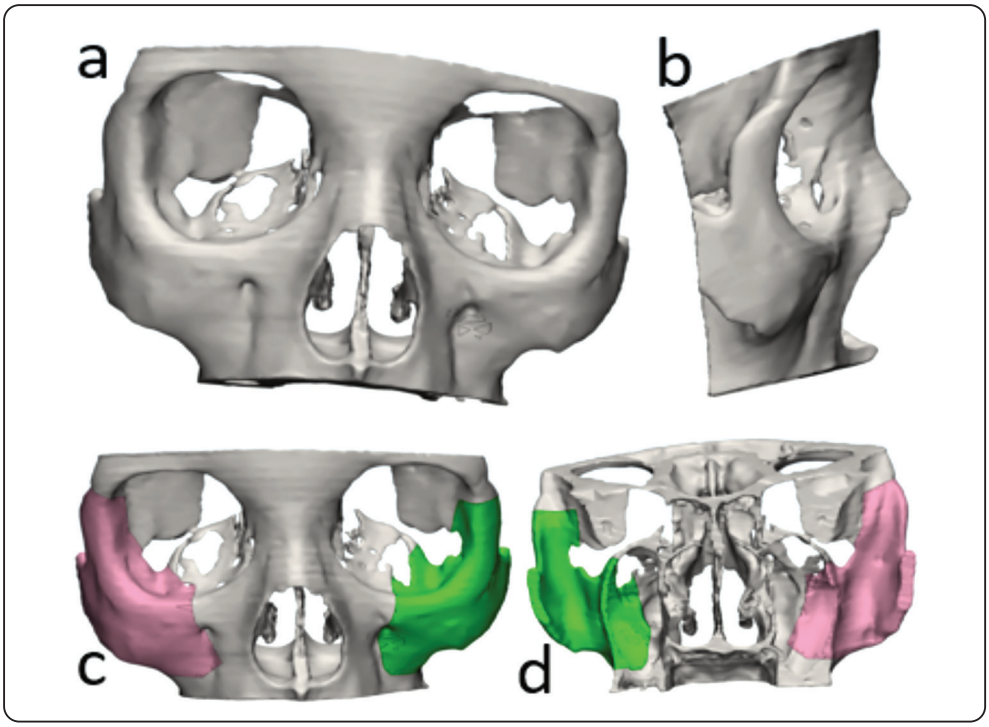

Fig. (3) a, b: full skull model frontal and lateral views; c, d: segmented zygomatic bones frontal and posterior views.

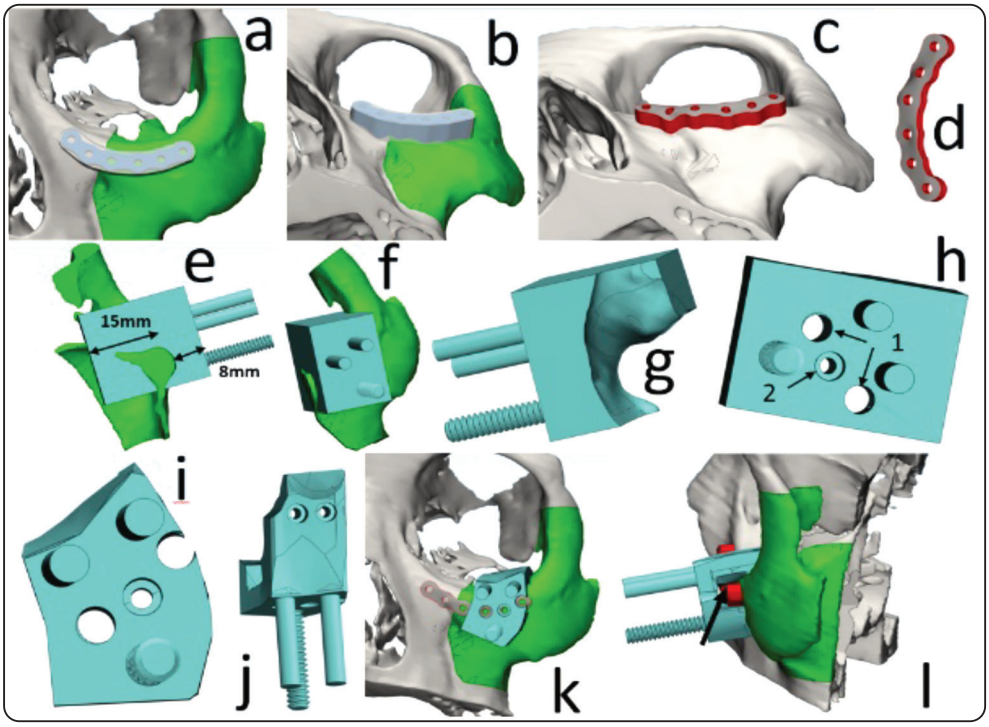

Fig. (4) a & b: IO-PT and IO-PT-ST placed parallel to and 4mm off the facial surface of the IOR; c & d: subtracted IO-PT adjusted to 3mm thickness; e & f: 3DP-ZSSG-MP base placed parallel to and 8mm off the facial surface of the IOR extended 15mm into the orbital cavity. The two guiding cylinders and the TCT oriented in a triangular pattern; g: 3DP-ZSSG-MP subtracted from the fractured zygoma duplicate; h: the two full depth 3.5mm diameter holes (1) and the first IOR-FS-SFS hole (2); i: the trimmed 3DP-ZSSG-MP; j: the two IOR-OS-SFS holes; k & l: IO-PT-ST duplicate subtracted of the 3DP-ZSSG-MP creating IO-P track (arrow).

Creation of 3DP-ZSSG:

3DP-ZSSG mobile part (3DP-ZSSG-MP): A cuboid (20LX15WX25Hmm^3) was oriented parallel to and 8mm off the IOR facial surface and with the orbital extension of 15mm. Two guiding cylinders (3mm diameter, 17mm height) and the TCT were placed perpendicular to the cuboid facial face in a triangular pattern creating the three-guiding columns (3GC). The four parts were fused to 3DP-ZSSG-MP. The 3DP-ZSSG-MP was subtracted from the fractured zygoma. Three facial holes corresponding to IO-P holes and two orbital holes were made. The two lateral facial and the middle holes were made with a 3.5mm full-depth, and 3.5mm 2mm-depth and 2mm-full-depth diameters, respectively, creating the first IOR-facial-surface stent-fixing screw (IOR-FS-SFS) and the two mobile part IOR-orbital-surface stent-fixing screws (IOR-OS-SFSs) holes. The 3DP-ZSSG-MP was trimmed to the bone contour. IO-PT-ST was subtracted from the 3DP-ZSSG-MP to create the IO-P track. (Fig4(e-l)) 3DP-ZSSG Fixed part (3DP-ZSSG-FP) designing: A cuboid (40LX25WX35H mm^3) was oriented parallel to and 4mm above the intact medial part of the IOR. A second cuboid fitted to the 3DP-ZSSG-MP facial face was subtracted from the first cuboid creating the 3DP-ZSSG-FP base. The 3DP-ZSSG-FP base was trimmed to the required shape and subtracted from the skull, the 3DP-ZSSG-MP, and the IO-PT-ST. Six facial holes corresponding to IO-P holes and two orbital holes were made. The second medial facial and the two orbital holes were made 3.5mm diameter at 2mm depth and 2mm to full depth, creating the second IOR-FS-SFS and the two fixed-part IOR-OS-SFS holes. The remaining holes were made with a 3.5mm full-depth diameter (Fig5a-f). The same was done for the opposite side. The broken skull, the two zygomas, and the two sides IO-P, ZF-P, and 3DP-ZSSGs were exported as STL files.

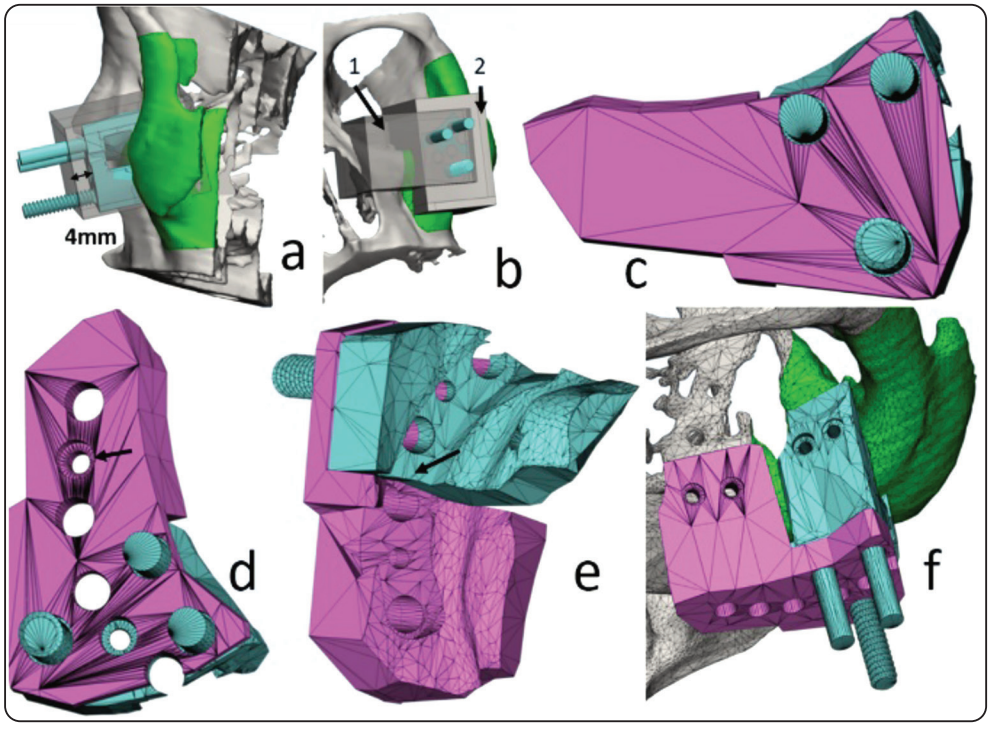

Fig. (5) a: The first cuboid oriented parallel to and 4mm off the facial surface of 3DP-ZSSG-MP; b: the first cuboid (1), the second cuboid fitted to the facial surface of 3DP-ZSSG-MP (2); c: 3DP-ZSSG-FP fixed part base trimmed to shape and subtracted off the skull, 3DP-ZSSG-MP duplicates and of the IO-PT-ST; d: six holes of 3DP-ZSSG-FP corresponding to IO-P with the second IOR-FS-SFS hole (arrow); e: the fitting surface of the 3DP-ZSSG showing the IO-P track (arrow); f: fully assembled 3DP-ZSSG showing the mobile (turquoise) and fixed part (magenta).

Printing process:

The STL models were imported for slicing to the Photon workshop (v 2.1.29). Automatic supports were created, and the models were sliced at 0.05mm-layer thickness. The sliced files were printed by Anycubic Photon Mono X 6K LCD-based 3D desktop printer (Anycubic-Griesheim-Gustav burg, Frankfurt, Germany) utilizing ABS-like photopolymer resin (SHENZHEN ELEGOO Technology CO., Ltd, Shenzhen**,** China). The prints were washed in an ultrasonic cleaner (Intelligent Ultrasonic Cleaner -600 mL-China) at 50-Watt power for 10 minutes using Isopropyl Alcohol 99.9%. The washed prints were solidified in UV Resin *Curing Light Box* (405nm UV led light with 360° Turntable).

Fracture reduction:

The 3DP-ZSSG-MP was aligned to the broken zygoma. Holes were drilled into the IOR using a 1.2mm drill (*Dremel*, Wisconsin, US) on a straight handpiece (*Dremel*, Wisconsin, US), and the 3DP-ZSSG-MP was fixed using micro screws (1.6mm diameter, 12mm length) (*LYJEE PA*, Letool international ltd). The 3DP-ZSSG-FP fixed part was inserted into the 3GC and aligned to the intact IOR. The 3DP-ZSSG-FP was drilled and screwed in position. The nut was screwed using the nut driver, slowly reducing the fractured zygoma into the planned position. ZF-P was seated in position, drilled, and screwed. The two IOR-FS-SFS were removed, keeping the four IOR-OS-SFSs fixing the 3DP-ZSSG and stabilizing the fractured zygoma. The IO-P was inserted into the IO-P track and fixed in position by reinserting the two IOR-FS-SFSs. The remaining four IO-P holes were drilled and screwed. The 3DP-ZSSG fixing screws and the 3DP-ZSSG were removed. The two IOR-FS-SFSs were reinserted in position (Fig. 6a-f&7a-c).

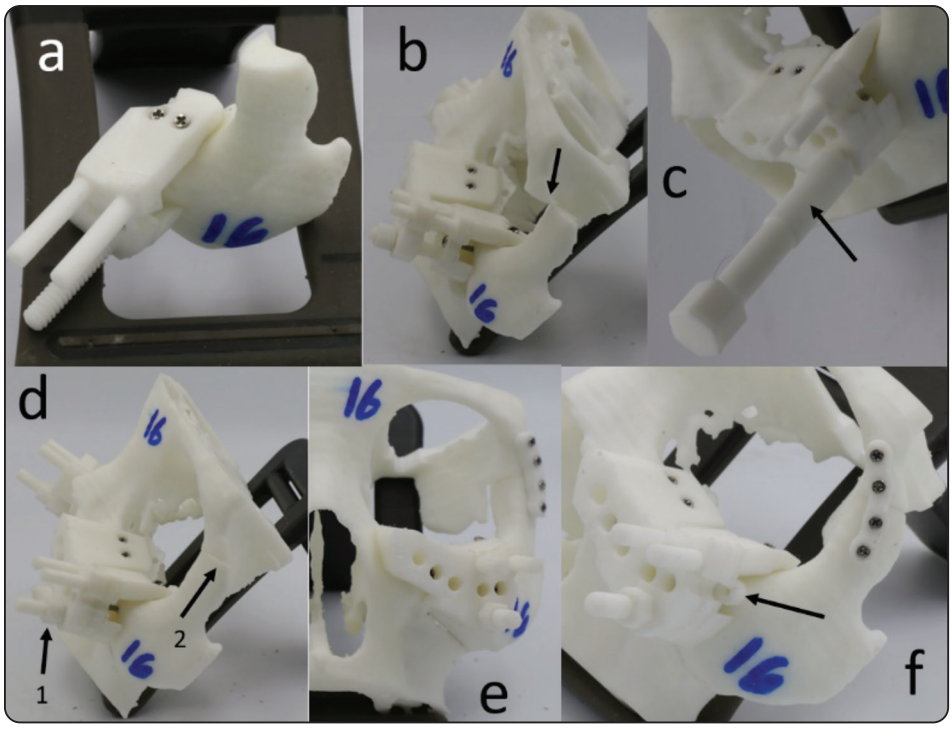

Fig. (6) a: 3DP-ZSSG-MP fixed to the broken zygoma using the two IOR-OS-SFS and the first IOR-FS-SFS; b: 3DP-ZSSG-FP assembled to the 3DP-ZSSG-MP, seated and fixed to the intact part of the IOR using the two IOR-OS-SFS and the second IOR-FS-SFS. The broken zygoma is not reduced into position (arrow); c: screwing the nut into place using nut driver (arrow); d: the nut screwed to the final position (1) actively reducing the zygoma into position (2); e: ZF-P fixed in position; f: the first and second IOR-FS-SFS were removed to allow the insertion of the IO-P (arrow) into the IO-P track.

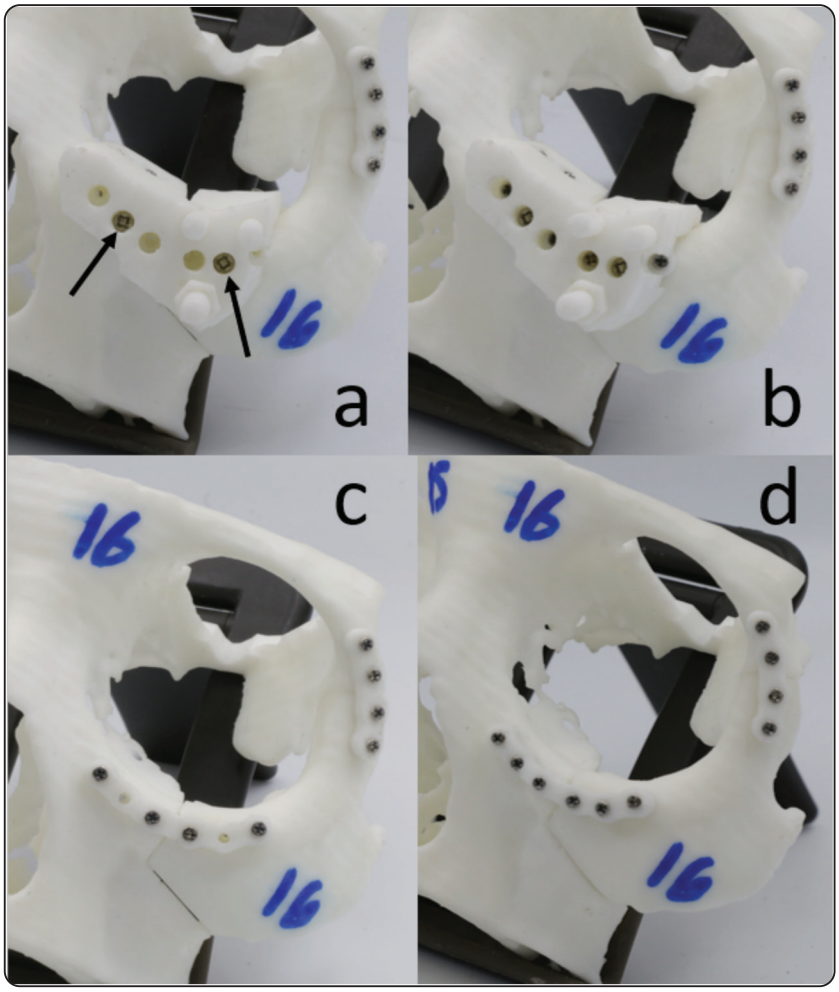

Fig. (7) a: The IO-P was fixed in position by reinserting the two IOR-FS-SFS (arrows); b: the remaining four IO-P holes were drilled, and the fixing screws were inserted; c: the 3DP-ZSSG was removed; d: the two IOR-FS-SFS reinserted in position.

Evaluation of zygomatic bone reduction:

Each reduced skull was scanned using an *Einscan SP scanner (SHINING 3D, Hangzhou, China)*, then imported to the corresponding *3-Matic file*. The scanned-reduced skull was aligned to the original skull using point registration followed by global automatic alignment. The assessment of zygomatic bone reduction was done through the following. Part surface comparison analysis: non-signed part-surface comparison analysis measured the maximum distance and the mean part-surface differences. Deviation at different zygomatic tails: The anterior and downward deviations at the IOR fracture were measured. Three standardized sectioning horizontal planes were made by cutting the skull at the mid-lateral orbital wall (section one), the infraorbital foramen (section two), and the lower part of the ZM fracture line (section three). Section one measured the anterior and medial deviations at ZFT and lateral deviation at the zygomaticosphenoidal tail (ZST). Section two measured lateral and anterior deviations at the zygomaticotemporal tail (ZTT). Section three measured the zygoma facial surface (FS-Z) anterior deviation at the ZM fracture line. The anterior and downward deviations at the IOR fracture were measured. (Fig8(a-f))

Statistical assessment

The mean, standard deviation, and minimal and maximum values were determined using Microsoft Excel 365.

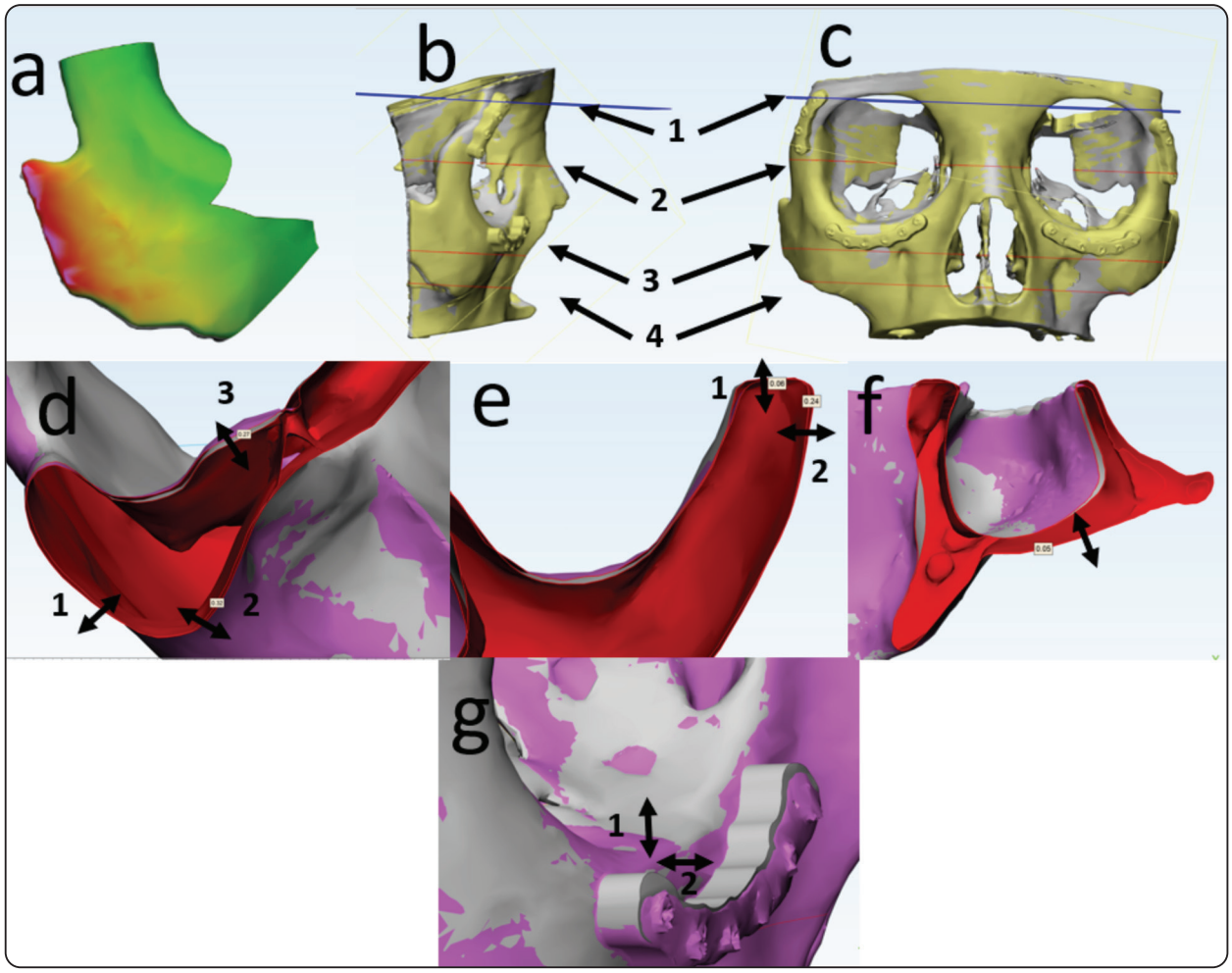

Fig. (8) a: Part surface comparison analysis; b & c: the horizontal plane (1), section one passing through the mid-lateral orbital wall (2), section two passing through the infraorbital foramen (3), and section three passing through the ZM fracture line (4); d: anterior and lateral deviations of ZFT (1 & 2, respectively), lateral deviation of ZST (3); e: anterior and lateral deviations of ZTT (1 & 2, respectively); f: anterior deviation of the FS-Z; g: downward and anterior deviation at the IOR fracture (1 & 2, respectively).

RESULTS

Evaluation of zygomatic bone reduction:

Table (1) describes the mean, standard deviation, maximum and minimum values of part surface analysis with a mean maximum comparison distance of 0.78±0.13mm and mean comparison distance of 0.16±0.14mm. Table (2) describes the reduction deviations at different zygomatic bone tails. The maximum mean deviation was the lateral deviation at ZTT of 0.60±0.39mm. There were no post-reduction deviations at IOR (anterior and downward) and ZFT (anterior direction).

TABLE (1) Part surface comparison analysis findings

	Maximum surface part comparison (mm)	Mean surface part comparison distance (mm)
Mean ± SD	0.78 ± 0.13	0.16 ± 0.14
Max Value	0.98	0.24
Min Value	0.58	0.12

TABLE (2) Reduction deviations at different zygomatic bone tails (mm).

Site	ZFT		ZTT		FS-Z	ZST	IOR	
Direction of displacement	Anterior	Medial	Anterior	Lateral	Anterior	Lateral	Anterior	Downward
Mean	0.00	0.32	0.41	0.60	0.29	0.22	0.00	0.00
SD	0.00	0.24	0.29	0.39	0.27	0.16	0.00	0.00
Max	0.00	0.93	0.93	1.49	0.96	0.56	0.00	0.00
Min	0.00	0.00	0.00	0.00	0.00	0.00	0.00	0.00

DISCUSSION

Zygomatic bone has complicated anatomical articulations affecting the nature and management of the ZMCFs. [2,9,26-28] Proper reduction is mandatory in the ZMCFS management. Minor reduction errors may cause functional and esthetic complications requiring secondary surgical intervention.[17,29] Utilizing local flaps during bone reduction does not allow the proper 3D perception of ZMC anatomy. Combining this poor 3D perception with surgeon mental simulation could lead to poor postoperative results.[9,14-16] Besides, reduction at ZST and ZTT is done indirectly utilizing these local flaps.[30] The availability of computer-aided surgical techniques for diagnosis, virtual planning, and treatment of maxillofacial fractures allowed for individualized surgical fracture treatment minimizing the potential of postoperative pitfalls.[13,18,31]

The 3DP-ZSSG managed to actively reduce the zygomatic bone into the virtually planned position with minimal mean deviation (ranging from zero to 0.6mm). This could be attributed to several reasons: 1) The three-dimensional spatial guidance of the 3GC's triangular orientation allowed 3D positioning of the zygomatic bone. 2) Facial and orbital extensions of the fixed and mobile parts allowed a broader surface of bone contact allowing for accurate guide positioning. Meanwhile, the 15mm extension of the guide into the orbit was within the safe orbital dissection distance (39.4±2.9mm from the IOR)[32], not extending to the inferior orbital fissure. 3) Inserting IO-P into position while keeping 3DP-ZSSG fixed to the bone stabilizes the zygomatic bone during plate drilling and screwing. 4) Stabilizing the individualized IO-P during drilling in the planned position using the two IOR-FS-SFSs prevents plate movement over the poor-anatomical-landmark facial surface of the IOR [24], which led to zero deviation at IOR. The current study also introduced a simple method for displacement evaluation that allows 3D perception of the zygomatic bone displacement in space, which could be used as a standardizing method for comparing different research.

Comparing the current study results to other studies is difficult due to the significant difference in the design and the evaluation parameters among the literature.[17] However, the comparison could indicate the reduction accuracy of ZMCFs utilizing 3DP-ZSSG. Clemens Klug et al.[33] utilized surgical simulation on 3D printed skull models and navigation system to reduce zygomatic fractures in 4 patients with screws position discrepancy of 1.1±0.3mm in the 3D coordinates. Feng et al.[34] bent the metal plates on 3D printed head models. They created self-cured acrylic resin surgical guides for the reduction of unilateral ZMCFs in 4 patients. Postoperative displacements were at the IOR (anteroposterior:2.11mm, up-down: 0.24mm), FS-Z (anteroposterior:1.14mm), ZTT (mediolateral:0.14mm, anteroposterior:2.01mm), and ZFT (mediolateral: 0.5mm, anteroposterior: 0.75mm). Li et al.[25] utilized individualized surgical

guides constructed using a rapid prototyping machine to reduce simulated ZMCFs in 6 cadaver heads. However, Li et al. did not specify the degree of deviation. Moreover, the design of their surgical guides required extensive exposure to the fracture sites and did not include a mechanism to guide the preformed plates' position.

Li et al. [35] in 2012 corrected an old zygomatico-orbito-maxillary fracture in a patient using virtual planning. The reduced skull and three surgical guides were 3D-printed, and the metal plates were bent over the printed skull. Li et al. reported consistent post-reduction anatomy but did not reveal the method of consistency determination. Moreover, Le et al. showed a 2.0mm deviation without clarifying the measurement method or the direction of variation.

Yang et al.[36] held a retrospective study on unilateral displaced zygomatic fractures comparing navigation assisted versus traditional reduction. The gaps at the sutures were as follows; ZTT (navigation:3.31±4.38mm, control:3.99±4.48mm), ZMT (navigation: 6.9±3.09mm, control: 5.13± 3.44mm), ZFT (navigation: 0.98±1.48mm, control: 2.01±1.95mm), and IOR (navigation:5.84±3.07mm, control:3.48 ± 3.41mm). Degala et al. [37] conducted a study to compare the two vs. three-point fixation of the unilateral ZMCFs following manual anatomical reduction. The two-point fixation of the first group was at ZFT and ZM buttress, adding a third point in the second group at IOR. The mean postoperative displacement at ZM buttress (group A:1.08mm, group B:0.33mm), IOR (group A:1.75mm, group B:0.42mm), and at FZT (group A:0.67mm, group B:0mm). Degala et al. did not clearly define the direction of displacement nor the standard deviation of the mean values. The current study utilized two points of fixation of ZMCFs at IOR and FZT. However, the present study's results were comparable to the three-point fixation group of the Degala et al. study, even better at the IOR.

Chu et al. [38] utilized a surgical navigation system to reduce unilateral ZMCFs in fifteen patients. Deviations corresponding to the current study measurements were as follows; FS-Z anteroposterior deviation (mean:0.69mm, max:2mm, min:0mm), ZTT mediolateral deviation (mean:0.71mm, max:1.5mm, min:0.2mm). Van Hout et al. [39] assessed the accuracy of ZMCFs treatment utilizing the intraoperative CBCT imaging following closed or opened reduction. Reduction revision was performed in cases of inadequate anatomical position. The postoperative mean surface-distance-difference between the reduced and the mirrored intact zygomas was 1.67±0.89mm.

3DP-ZSSG is a valuable innovative tool for the active reduction of ZMCFs. The deviations of the reduced zygoma from the planned position using the 3DP-ZSSG were minimal compared to the results of compared studies. The design of the 3DP-ZSSG has the flexibility for modification specific to every case. The basic idea is to attach the fixed part to the suitable intact bone and the mobile part to the fractured segment. This concept could be applied in the reduction of other facial bone fractures. Moreover, the stable-wide fixation of the mobile part to the fractured piece allowed easy manipulation of the broken bone, declining the need for other manipulating tools such as the Carroll Girard screw. Besides, the size of the assembled guide (mediolateral length of 3cm, up-down height of approximately 1cm at the medial end, 2cm at the lateral end) could be accommodated by subconjunctival or subciliary incisions with lateral canthotomy. 3D-printed surgical guides are cheaper, easy to use, require less intraoperative preparation time, and need minimal gear.[24,40]

However, the 3DP-ZSSG requires the basic skills of using 3D designing software. Though the potential of 3DP-ZSSG usage in ZMCFs is limitless, improving the learning curve deserves to be done. The application of 3DP-ZSSG in vivo is required to examine clinical cases' usability.

Funding: None.

Competing interests: no conflicts of interest.

Ethical approval: Not required.

REFERENCE

1. Lin Q, Hong XY, Zhang D, Jin HJ. Preoperative evaluation and surgical technique of functional and cosmetic aspects in zygomatic complex fracture patients. J Biol Regul Homeost Agents 2017:31:1005-1012.
2. Swetaa A, Babu KY, Mohanraj KG. Zygomatic complex fracture - A review. Drug Invention Today 2018:10:3058-3061.
3. Iwanaga H, Nuri T, Ueda K. Comparison of the Biomechanical Stiffness of Titanium and Sonic Weld RX Osteofixation Systems for Monoblock Zygomaticomaxillary Complex Fractures. J Craniofac Surg 2021:32:1549-1552. doi: 10.1097/scs.0000000000007167.
4. Chu H, Chu Y, Xu X. Minimally Invasive Treatment With Zygomatic Complex Fracture Reduction by Percutaneous Bone Hook Traction. J Oral Maxillofac Surg 2021:79:1514-1527. doi: 10.1016/j.joms.2021.02.011.
5. Mishra P, Khan P, Salunkhe SM, Pendyala SK, Mathur M, Ummadisingh L, et al. Factors Affecting Quality of Life in Zygomatic Fractures: An Original Research. J Pharm Bioallied Sci 2022:14:S242-S244. doi: 10.4103/jpbs.jpbs_702_21.
6. Xing Z, Ren R, Xia X, Yang L. Supra-Temporalis Approach for Treating Zygomaticomaxillary Complex Fracture. J Craniofac Surg 2021:32:1087-1089. doi: 10.1097/SCS.0000000000007463.
7. Yamsani B, Gaddipati R, Vura N, Ramisetti S, Yamsani R. Zygomaticomaxillary Complex Fractures: A Review of 101 Cases. J Maxillofac Oral Surg 2016:15:417-424. doi: 10.1007/s12663-015-0851-9.
8. Boffano P, Roccia F, Gallesio C, Karagozoglu KH, Forouzanfar T. Infraorbital nerve posttraumatic deficit and displaced zygomatic fractures: a double-center study. J Craniofac Surg 2013:24:2044-2046. doi: 10.1097/SCS.0b013e3182a41c9d.
9. Birgfeld CB, Mundinger GS, Gruss JS. Evidence-Based Medicine: Evaluation and Treatment of Zygoma Fractures. Plast Reconstr Surg 2017:139:168e-180e. doi: 10.1097/PRS.0000000000002852.
10. Zingg M, Laedrach K, Chen J, Chowdhury K, Vuillemin T, Sutter F, et al. Classification and treatment of zygomatic fractures: a review of 1,025 cases. J Oral Maxillofac Surg 1992:50:778-790. doi: 10.1016/0278-2391(92)90266-3.
11. Lee EI, Mohan K, Koshy JC, Hollier LH, Jr. Optimizing the surgical management of zygomaticomaxillary complex fractures. Semin Plast Surg 2010:24:389-397. doi: 10.1055/s-0030-1269768.
12. Peretti N, MacLeod S. Zygomaticomaxillary complex fractures: diagnosis and treatment. Curr Opin Otolaryngol Head Neck Surg 2017:25:314-319. doi: 10.1097/moo.0000000000000372.
13. Strong EB, Gary C. Management of Zygomaticomaxillary Complex Fractures. Facial Plast Surg Clin North Am 2017:25:547-562. doi: 10.1016/j.fsc.2017.06.006.
14. Schneider M, Besmens IS, Luo Y, Giovanoli P, Lindenblatt N. Surgical management of isolated orbital floor and zygomaticomaxillary complex fractures with focus on surgical approaches and complications. J Plast Surg Hand Surg 2020:54:200-206. doi: 10.1080/2000656X.2020.1746664.
15. Cuddy K, Dierks EJ, Cheng A, Patel A, Amundson M, Bell RB. Management of Zygomaticomaxillary Complex Fractures Utilizing Intraoperative 3-Dimensional Imaging: The ZYGOMAS Protocol. J Oral Maxillofac Surg 2021:79:177-182. doi: 10.1016/j.joms.2020.08.028.
16. van Hout WM, Van Cann EM, Koole R, Rosenberg AJ. Surgical treatment of unilateral zygomaticomaxillary complex fractures: A 7-year observational study assessing treatment outcome in 153 cases. J Craniomaxillofac Surg 2016:44:1859-1865. doi: 10.1016/j.jcms.2016.09.002.
17. Dubron K, Van Camp P, Jacobs R, Politis C, Shaheen E. Accuracy of virtual planning and intraoperative navigation in zygomaticomaxillary complex fractures: A systematic review. J Stomatol Oral Maxillofac Surg 2022:123:e841-e848. doi: 10.1016/j.jormas.2022.07.003.
18. Chen X, Lin Y, Wang C, Shen G, Zhang S, Wang X. A surgical navigation system for oral and maxillofacial surgery and its application in the treatment of old zygomatic fractures. Int J Med Robot 2011:7:42-50. doi: 10.1002/rcs.367.
19. Huang D, Chen M, He D, Yang C, Yuan J, Bai G, et al. Preservation of the inferior alveolar neurovascular bundle in the osteotomy of benign lesions of the mandible using a digital template. Br J Oral Maxillofac Surg 2015:53:637-641. doi: 10.1016/j.bjoms.2015.04.013.
20. Lin L, Liu X, Gao Y, Aung ZM, Xu H, Wang B, et al. The application of augmented reality in craniofacial bone fracture reduction: study protocol for a randomized controlled trial. Trials 2022:23:1-10. doi: 10.1186/s13063-022-06174-3.
21. Du W, Yang M, Liu H, Ji H, Xu C, Luo E. Treatment of hemimandibular hyperplasia by computer-aided design and computer-aided manufacturing cutting and drilling guides accompanied with pre-bent titanium plates. J Craniomaxillofac Surg 2020:48:1-8. doi: 10.1016/j.jcms.2019.01.039.

22. Zhang C, Ma MW, Xu JJ, Lu JJ, Xie F, Yang LY, et al. Application of the 3D digital ostectomy template (DOT) in mandibular angle ostectomy (MAO). J Craniomaxillofac Surg 2018:46:1821-1827. doi: 10.1016/j.jcms.2018.07.026.
23. Yang WF, Choi WS, Leung YY, Curtin JP, Du R, Zhang CY, et al. Three-dimensional printing of patient-specific surgical plates in head and neck reconstruction: A prospective pilot study. Oral Oncol 2018:78:31-36. doi: 10.1016/j.oraloncology.2018.01.005.
24. Zhao L, Zhang X, Guo Z, Long J. Use of modified 3D digital surgical guides in the treatment of complex mandibular fractures. J Craniomaxillofac Surg 2021:49:282-291. doi: 10.1016/j.jcms.2021.01.016.
25. Li J-p, Chen S-l, Zhang X, Chen X-y, Deng W. Experimental Research of Accurate Reduction of Zygomatic-Orbitomaxillary Complex Fractures with Individual Templates. J Oral Maxillofac Surg 2011:69:1718-1725. doi: 10.1016/j.joms.2010.09.006.
26. Knight JS, North JF. The classification of malar fractures: An analysis of displacement as a guide to treatment. Br j Plast Surg, 1961:325-339.
27. Rohrich RJ, Watumull D. Comparison of rigid plate versus wire fixation in the management of zygoma fractures: a long-term follow-up clinical study. Plast Reconstr Surg 1995:96:570-575. doi: 10.1097/00006534-199509000-00008.
28. Manson PN, Clark N, Robertson B, Slezak S, Wheatly M, Vander Kolk C, et al. Subunit principles in midface fractures: the importance of sagittal buttresses, soft-tissue reductions, and sequencing treatment of segmental fractures. Plast Reconstr Surg 1999:103:1287-1306; quiz 1307.
29. Jazayeri HE, Khavanin N, Yu JW, Lopez J, Shamliyan T, Peacock ZS, et al. Fixation Points in the Treatment of Traumatic Zygomaticomaxillary Complex Fractures: A Systematic Review and Meta-Analysis. J Oral Maxillofac Surg 2019:77:2064-2073. doi: 10.1016/j.joms.2019.04.025.
30. Khojastepour L, Razavi N, Hasani M, Khaghaninejad MS. Evaluation of Zygomaticosphenoidal Angle in Patients With Unilateral Zygomaticomaxillary Complex Fracture. J Craniofac Surg 2022:33:e370-e373. doi: 10.1097/SCS.0000000000008159.
31. Zachow S, Hege H-C, Deuflhard P. Computer Assisted Planning in Cranio-Maxillofacial Surgery. J Comput Inform Tech 2006:14:53-64. doi: 10.2498/cit.2006.01.06.
32. Danko I, Haug RH. An experimental investigation of the safe distance for internal orbital dissection. J Oral Maxillofac Surg 1998:56:749-752-752. doi: 10.1016/S0278-2391(98)90812-6.
33. Klug C, Schicho K, Ploder O, Yerit K, Watzinger F, Ewers R, et al. Point-to-Point Computer-Assisted Navigation for Precise Transfer of Planned Zygoma Osteotomies from the Stereolithographic Model into Reality. J Oral Maxillofac Surg 2006:64:550-559. doi: 10.1016/j.joms.2005.11.024.
34. Feng F, Wang H, Guan X, Tian W, Jing W, Long J, et al. Mirror imaging and preshaped titanium plates in the treatment of unilateral malar and zygomatic arch fractures. Oral Surg Oral Med Oral Pathol Oral Radiol Endod 2011:112:188-194. doi: 10.1016/j.tripleo.2010.10.014.
35. Li P, Tang W, Li J, Tian DW. Preliminary application of virtual simulation and reposition template for zygomatico-orbitomaxillary complex fracture. J Craniofac Surg 2012:23:1436-1439-1439. doi: 10.1097/SCS.0b013e318260edde.
36. Yang C, Lee MC, Pan CH, Chen CH, Chen CT. Application of Computer-Assisted Navigation System in Acute Zygomatic Fractures. Ann Plast Surg 2019:82:S53-s58. doi: 10.1097/sap.0000000000001721.
37. Degala S, Radhakrishna S, Dharmarajan S. Zygomaticomaxillary fracture fixation: a prospective comparative evaluation of two-point versus three-point fixation. Oral Maxillofac Surg 2021:25:41-48. doi: 10.1007/s10006-020-00881-4.
38. Chu Y-Y, Yang J-R, Lai B-R, Liao H-T. Preliminary outcomes of the surgical navigation system combined with intraoperative three-dimensional C-arm computed tomography for zygomatico-orbital fracture reconstruction. Sci Rep 2022:12:1-14. doi: 10.1038/s41598-022-11659-x.
39. van Hout WMMT, de Kort WWB, ten Harkel TC, Van Cann EM, Rosenberg AJWP. Zygomaticomaxillary complex fracture repair with intraoperative CBCT imaging. A prospective cohort study. J Craniomaxillofac Surg 2022:50:54-60. doi: 10.1016/j.jcms.2021.09.009.
40. Aboul-Hosn Centenero S, Hernández-Alfaro F. 3D planning in orthognathic surgery: CAD/CAM surgical splints and prediction of the soft and hard tissues results - our experience in 16 cases. J Craniomaxillofac Surg 2012:40:162-168. doi: 10.1016/j.jcms.2011.03.014.